

# Smooth Vortex Precession in Superfluid $^4\text{He}$

L. Hough, L.A.K. Donev, and R.J. Zieve

*Physics Department, University of California at Davis*

We have measured a precessing superfluid vortex line, stretched from a wire to the wall of a cylindrical cell. By contrast to previous experiments with a similar geometry, the motion along the wall is smooth. The key difference is probably that our wire is substantially off center. We verify several numerical predictions about the motion, including an asymmetry in the precession signature, the behavior of pinning events, and the temperature dependence of the precession.

PACS numbers: 47.32.Cc, 47.37.+q, 67.40.Vs

## I. INTRODUCTION

Vortices appear in systems from superconductors and superfluids to weather patterns and blood flow [1]. They underlie complex fluid flows, and motivate computational techniques [2, 3]. Measurements of the behavior of one or a few vortices provide test cases for computations and starting points for understanding more complicated vortex systems. Indeed, even small numbers of vortices can produce interesting dynamics, such as the hopscotch motion of two coaxial vortex rings [4]. Yet in classical systems, even *defining* a single vortex can be difficult [5]. For example, in a classical fluid the vorticity fields of two nearby vortices may overlap and resemble a single vortex.

By contrast, a superfluid vortex is well-defined, since circulation is quantized and non-zero vorticity occurs only within the vortex core. In superfluid  $^4\text{He}$ , the core size is only a few angstroms, and vortices closely approximate the ideal slender vortices of theoretical treatments. Although in principle superfluid experiments can verify theoretical and computational models of vortex dynamics, few measurements can probe individual vortex behavior. Two exceptions are the observation of a precessing vortex in a Bose-Einstein condensate [6] and diffraction experiments on superconducting vortices [7]. However, these techniques have limitations for dynamical studies, the former because of the condensate lifetime and the latter because of the time for each measurement. Here we discuss a different experiment, which detects single vortex motion in superfluid helium.

Our apparatus consists of a straight wire, stretched along a cylinder. A current pulse in a perpendicular magnetic field makes the wire vibrate. The subsequent motion perpendicular to the field is detected as a voltage across the wire. In the presence of fluid circulating around the wire, the normal modes of the wire's vibration are split, with the beat frequency revealing the circulation around the wire. This technique originated nearly forty years ago in early measurements of quantized circulation in superfluid  $^4\text{He}$  [8, 9], and was later used to measure circulation in superfluid  $^3\text{He}$  [10].

A question that persisted through two decades of vibrating wire measurements is why intermediate circulation values are

frequently observed. The expected quantum levels are clearly more stable, but other values occur as well. One suggestion was that a vortex might run along the wire for only part of the wire's length, then detaching and becoming a free vortex in the fluid, terminating on the cell wall. This results in a partial effect on the vibration frequencies, as would fractional circulation along the entire length of the wire. Recently this idea was verified, originally in superfluid  $^3\text{He}$  [11, 12]. The free end of a partially trapped vortex precesses about the wire, driven by the flow field of the trapped portion. If the wire is displaced from the axis of the cell, the precession appears in the beat frequency as oscillations.

A similar effect was observed in  $^4\text{He}$ , with the same cell used for the  $^3\text{He}$  measurements, although noise in the attachment point motion usually hid any oscillations present [13]. Even the cleanest  $^4\text{He}$  signal was far more irregular than a typical  $^3\text{He}$  signature. Furthermore, the earlier generations of vibrating wire measurements in  $^4\text{He}$  found no recognizable precession signature. One possible explanation of the difference in signals is the much smaller vortex core radius: 1.3 Å in  $^4\text{He}$  as opposed to 1000 Å in  $^3\text{He}$ . The smaller core makes the  $^4\text{He}$  vortex more sensitive to roughness on the surface of the cell and the wire. Given the difficulty of experiments on rotating superfluid  $^3\text{He}$ , particularly vibrating wire experiments that must be carried out well below the 2 mK transition temperature, and the appeal of further measurements on a single vortex line undergoing a fundamentally three dimensional motion, we returned to  $^4\text{He}$  to attempt to resolve a smoother signature there.

Here we report smooth vortex precession in  $^4\text{He}$ . In the process of this work, we have verified several numerical predictions about the details of the motion [14], which were inspired by the original  $^3\text{He}$  work.

## II. EXPERIMENTAL BACKGROUND

Our experimental setup is similar to that used in previous generations of vibrating wire experiments [8, 9, 13]. A brass cylinder of height 50 mm and inner radius about 1.5 mm is filled with helium. A NbTi wire a few microns in radius

is stretched parallel to the cylinder's axis, entering the cell through Stycast 1266 caps with small holes displaced 0.3 to 0.5 mm from the axis. The wire is glued into the caps with a small weight hanging from it to keep it under tension.

In principle the wire should have doubly degenerate normal modes at its fundamental frequency. However, as explained in detail in Ref. [9], the modes are actually linear and perpendicular. They differ in frequency by  $\Delta\omega_0$ , probably because of imperfections in the wire's cross-section or mounting. If the wire serves as the core of a superfluid vortex with circulation  $\kappa$ , the normal modes become ellipses with major axes aligned with the original linear modes. The frequency splitting increases to

$$\Delta\omega = \sqrt{(\Delta\omega_0)^2 + \left(\frac{\rho_s \kappa}{\mu}\right)^2}, \quad (1)$$

where  $\rho_s$  is the superfluid density and  $\mu$  is the mass per length of the wire, adjusted for the fluid displaced during vibration. The lowest non-zero circulation is  $\kappa = \frac{h}{m}$ , with  $m$  the mass of a  $^4\text{He}$  atom. With  $\rho_s = 0.145 \text{ g/cm}^3$  and  $\mu \approx 15 \times 10^{-6} \text{ g/cm}$ , the frequency splitting from this circulation is  $\frac{\rho_s \kappa}{\mu} = 9.6 \text{ rad/s}$ .

The magnetic field, about 200 Oersted, comes from two saddle coil magnets. Changing their relative current rotates the field through the plane perpendicular to the wire. For detection purposes, a key point is that in general the wire does not move in a plane perpendicular to the magnetic field. Since the excitation method uses current in the wire and the resulting Lorentz force, the wire always *starts* moving perpendicular to the field; but vibration in this plane usually is not a normal mode. Instead the wire traces out an elaborate path, with its velocity at times nearly or entirely perpendicular to the magnetic field. The induced emf shows beats in the oscillation envelope at frequency  $\Delta\omega$ . Orienting the field halfway between the two linear normal modes excites the modes equally and leads to complete beats, with or without circulation around the wire.

The voltage signal goes to a 100:1 PAR 1900 transformer at room temperature, then to a Stanford Research Instruments SR560 pre-amplifier and SR830 lock-in amplifier. The oscillation magnitude is read to the computer through a 16-bit A/D board. In real time, we fit the envelope to an exponentially damped sine wave with four adjustable parameters (amplitude, phase, frequency, and damping). We also save the original digitized decays for possible re-analysis later. The accuracy in ascertaining the beat frequency varies from wire to wire. It depends heavily, for example, on the beat frequency itself. Typically we can extract the beat frequency to 0.1% below 400 mK. The uncertainty arises primarily from mechanical vibrations which shake the wire, rather than from electronic noise.

A partially trapped vortex has less effect on the wire's beat frequency. The beat frequency in this case depends on what part of the wire is covered with the vortex. Since the middle has a larger vibration amplitude than the ends, it contributes more heavily to the final beat frequency. If there is one quantum of circulation on the wire below an attachment point  $z$ , and zero circulation above  $z$ , then Equation 1 still holds, with

$\kappa$  replaced by an effective circulation  $\langle \kappa \rangle$  defined by [9]

$$\langle \kappa \rangle = \frac{1}{2L} \int_0^z \frac{h}{m} \sin^2 \frac{\pi}{L} z' dz' = \frac{h}{m} \left( \frac{z}{L} - \frac{1}{2\pi} \sin \frac{2\pi z}{L} \right). \quad (2)$$

Here  $L$  is the length of the wire, and we assume that the lowest normal modes are sinusoidal in the  $z$  direction.

The conversion from the total beat frequency to the contribution from circulation, Equation 1, is insensitive at values of  $\Delta\omega$  near  $\Delta\omega_0$ , where the wire's imperfections overwhelm the effect of circulation. The conversion from circulation to attachment point location, Equation 2, has low sensitivity near both  $\langle \kappa \rangle = 0$  and  $\langle \kappa \rangle = \frac{h}{m}$ . As a result, our measurements are mainly of the vortex moving in the middle of the cell, where our sensitivity lets us locate the attachment point to better than  $50 \mu\text{m}$ .

As mentioned previously, when a vortex is partially attached to the wire, the free end precesses about the wire. If the wire is displaced from the axis of the cylinder, the length of the free vortex changes as it moves. This would alter the energy in the flow field unless compensated by motion of the attachment point. We detect the attachment point motion as oscillations in the beat frequency of the wire.

Figure 1 shows the oscillations characteristic of the unwinding process. The two portions of the figure show data taken at different times but with the same cell. Each point represents a separate plucking of the wire. The oscillations correspond to the motion of the free vortex around the cell, and the gradual decay of the circulation happens because the moving vortex dissipates energy. Figure 1 also shows the qualitative distinction between the expected quantized circulation levels, which we will refer to by quantum number ( $n = 0, n = 1$ , etc.) and intermediate levels, both at  $n > 1$  and  $n < 1$ . The quantized levels are far more stable and exhibit none of

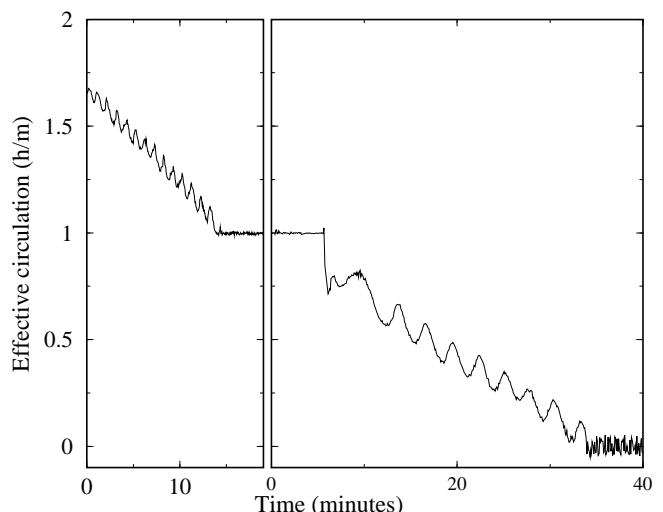


FIG. 1: Unwinding of vortex from wire. The two parts of the figure have the same horizontal scale.

TABLE I: Estimated dimensions for the five wires used here.

	$R$ (mm)	$R_W$ ( $\mu\text{m}$ )	$\omega$ (rad/s)	$\Delta\omega_o$ (rad/s)	Smallest $T$ (s)	Predicted $T$ (s)
A	1.4	5.1	6666	25.5	187	138
B	1.4	5.1	4115	3.02	—	138
C	1.4	8.9	2262	6.53	147	154
D	1.53	8.8	1929	10.3	171	180
E	1.53	8.6	1030	33.8	194	179

the oscillations due to precession. The increased noise near  $n = 0$  is inherent in the analysis equations, as mentioned above. Finally, the figure shows the different precession periods for decays at  $n > 1$  and  $n < 1$ , roughly one minute and three minute, respectively. In the former case the circulation around the wire is  $2\frac{h}{m}$  near one end and  $\frac{h}{m}$  near the other, with a singly quantized vortex emerging from the wire at the spot where the circulation changes. The flow field is that of three half-vortices, rather than one, so the vortex precesses three times as fast.

We discuss measurements on five wires, which are described in Table I. Each wire is a single strand cut from multistranded NbTi wire. By weighing several strands, and using  $6.0 \text{ g/cm}^3$  as the density of NbTi, we find that the average mass per length corresponds to a radius of  $5.1 \mu\text{m}$  for wires such as A and B, and  $8.7 \mu\text{m}$  for wires such as C, D, and E. For the wires that trap a stable  $n = 1$  vortex, we can take the observed stable beat frequencies as  $\Delta\omega$  and  $\Delta\omega_o$  in Equation 1 and find the mass per length of the wire. The corresponding radius values, shown in Table I, are close to the values found from the weights. For wires A and B, no stable  $n = 1$  state was seen, and Table I shows the radius calculated from the typical wire weight. As an additional check, the room temperature resistance of the wires should be proportional to cross-sectional area. The radius values in Table I are indeed consistent with the wires' resistances. As discussed below, the amplitude and shape of the oscillation signals depend on the displacement from the cylinder axis. Our observations are consistent with the displacements measured during assembly of the cells.

The measurements are performed on a pumped  $^3\text{He}$  cryostat with a minimum temperature of 250 milliKelvin. The cryostat has an external  $^4\text{He}$  pumping line, which passes through a rotating vacuum seal. For the experiments discussed here, all measurements are made with the cryostat stationary. We fill the cell at 4K, then cool into the superfluid. Once cold, we rotate by hand, typically 10 revolutions in one minute, to create circulation. During rotation our electrical wires are disconnected. When we restart the measurements, we usually find an unstable state, which can have circulation either larger or smaller than the  $n = 1$  state. If the circulation settles to a stable  $n = 1$  state, we dislodge the vortex by moving the cryostat rapidly about 60 degrees, in the direction opposite to the previous rotation direction, and then slowly returning it to its original position. This minimally controlled shaking generally results in one of two vortex signatures. Sometimes an abrupt drop in trapped circulation is followed by oscillations

indicating vortex precession. At other times, the circulation drops, but then increases back to  $n = 1$  in the characteristic, slightly irregular way illustrated several times in Figure 2. One possible explanation is that a portion of the vortex is dislodged from the wire, but does not reach the cell wall. The detached portion then precesses through the cell, spiraling inward until it is recaptured by the wire. We have not yet identified whether the detaching occurs near the center or end of the wire; schematics of these two possibilities are shown in Figure 2.

### III. COMPUTATIONAL BACKGROUND

To complement our experimental work, we do simulations of superfluid vortex dynamics. Our code is similar to that of Schwarz [14, 15], and is described elsewhere [16]. Here we briefly summarize its workings. The equations of motion for the vortex are based on the incompressible Euler equations, which would require the vortex core to move at exactly the local superfluid velocity. A friction term  $-\alpha\mathbf{s}' \times \mathbf{v}_s$  is added which gives the vortex motion an additional component perpendicular to the superfluid velocity. Here the friction coefficient  $\alpha$  determines the strength of the friction interaction;  $\mathbf{s}'$  is the tangent to the vortex line, directed so that the cir-

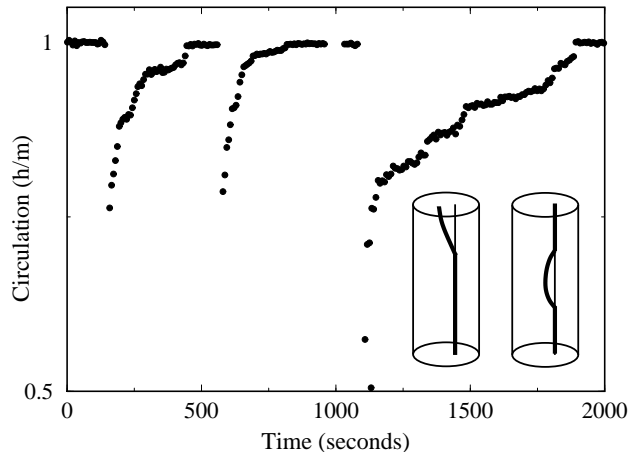


FIG. 2: Characteristic signal for vortex partly dislodging and returning to wire. The insets show two possibilities for the vortex configuration corresponding to the intermediate circulation values.

ulation is given from  $s'$  by the right-hand rule; and  $\mathbf{v}_s$  is the superfluid velocity. We calculate the fluid velocity from the instantaneous core locations and boundary conditions imposed by the cylindrical container. The vortex cores have a local contribution proportional to the vortex curvature, and a non-local contribution from distant segments which obeys the Biot-Savart law. For the present geometry, we neglect the latter except for the portion of the vortex trapped along the wire, which we treat as a half-infinite straight vortex. We meet the boundary conditions approximately using an image vortex: a second half-infinite vortex defined from the trapped vortex by inversion in the cylinder. Adding the image under inversion of the free vortex segment does not significantly change the results.

We use dimensions similar to those of the actual experiment: a cell of radius 1.5 mm, and a wire of radius  $6 \mu\text{m}$ . Near the wire the point spacing along the vortex is comparable to the wire radius, and it gradually increases with increasing distance from the wire.

#### IV. SMOOTH PRECESSION

In the absence of dissipation, the precession period for a single partially attached vortex is given by

$$T = \frac{4\pi^2(R^2 - R_W^2)}{\kappa \ln \frac{R}{R_W}}. \quad (3)$$

As shown in Table I, the predicted and actual values for our cells are in reasonable agreement, with typical precession periods slightly under three minutes. The discrepancies are larger than in  $^3\text{He}$  [11, 12] or in lower-temperature  $^4\text{He}$  [13] measurements. A major reason for this is that in our temperature range the precession period varies substantially with temperature. We discuss this behavior below.

We first address the smooth nature of the motion, not previously found in  $^4\text{He}$ . Four of the five wires show smooth precession signatures. With the fifth, wire B, circulation decays rapidly with no clean precession. These are the *only* wires we have measured, so the contrast with the noisy intermediate-circulation data from the previous experiments is striking. The one deliberate difference in our design is that, instead of trying to center the wire in the cylinder, we intentionally move it off the axis to increase the amplitude of the precession signal. We suggest that a displaced wire also leads to more regular vortex precession.

Hints that wire displacement can influence the smoothness of the precession first appear in Schwarz's simulations of a vortex precessing in a cylinder [14]. His calculations incorporate pinning, but without any geometrical details of the pin sites; rather, one end of the vortex is simply fixed in position. The local fluid velocity bends the vortex towards the wall. For depinning, Schwarz uses a critical angle model: when the angle between the vortex and the wall falls below a critical value, the fixed end of the vortex becomes free, and is once again allowed to move along the wall. If the critical angle is too small, the vortex never reaches it and remains pinned. To simulate

vortex precession with wall roughness, the chosen angle must be large enough that the vortex never becomes permanently pinned. Schwarz mentions that an off-center wire allows a smaller critical angle than an on-center wire [14]. This suggests that a vortex running from an off-center wire to the wall is better able to free itself from pin sites and continue its motion. Our present work gives some experimental confirmation of the critical angle model. The reduced pinning from putting the wire deliberately off center changes the signature from noisy to smooth.

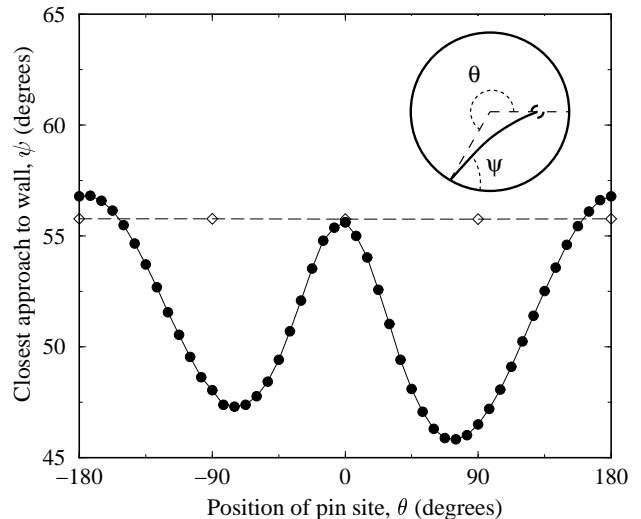


FIG. 3: Minimum angle from wall that occurs as vortex settles into pin site. The calculations use no friction ( $\alpha = 0$ ).  $\diamond$ : wire on cylinder axis.  $\bullet$ : wire displaced 0.4 mm from cylinder axis. The inset shows the geometry. The black dot represents the wire, which has counter-clockwise circulation on the portion away from the viewer. The solid arc is the free segment of the vortex. The angle  $\psi$  may not lie in the plane of the page.

Our own simulations on pinning in a cylinder provide more details. We begin by calculating the trajectory of a precessing vortex. Initially waves propagate along the vortex as it settles into the configuration appropriate for steady precession. Once these oscillations in the vortex shape have decayed away, we abruptly cease the motion of the endpoint on the wall. The vortex then again oscillates, settling gradually into a permanent position. We find the minimum angle with the wall achieved during this process, shown in Figure 3 for an on-center wire and one displaced 0.4 mm. The point spacing near the wall is  $53 \mu\text{m}$  for these calculations, corresponding to a bump size of  $23 \mu\text{m}$  [16]. As the wire becomes farther off center, the minimum angle decreases substantially at most locations in the cell, but increases slightly where the vortex is longest. Our interpretation is that a vortex coming from an off-center wire frees itself more easily from a pin site, for most locations of the pin site. However, it appears that near  $180^\circ$  the off-center wire actually makes depinning more difficult. Experimentally the smooth precession does not cease in this portion of the cell, so some further explanation

is required. One explanation is to model the wall roughness as bumps of different sizes, each with its own critical angle. Larger bumps, which pin vortices more easily, correspond to smaller critical angles. As long as the largest bumps lie outside the narrow region near  $180^\circ$  where the pinning is easier for the displaced wire than for the on-center wire, moving the wire off center may still reduce pinning. Another possibility is that encountering pin sites during precession alters the vortex shape, presumably bending the vortex line closer to the cell wall. Changing the configuration at the onset of a pinning event affects the minimum angle achieved, perhaps decreasing the off-center wire's minimum angle below that of the on-axis wire everywhere in the cell.

Several factors determine the angle the vortex attains after pinning. The flow velocity depends on the displacement of the wire from the cell axis, and also on the location of the free vortex in the cell. The velocity is faster where the wire approaches the cell wall more closely. In addition, if the wire is off center, a straight line from the wire to the cell wall is generally not perpendicular to the wall. This defines a natural angle for a vortex at any spot in the container. Although the vortex may curve, meeting the wall at a different angle, this simple geometrical consideration is a major factor in determining the final angle. Finally, the asymmetry visible between the two sides of the cell comes from the direction of the fluid flow relative to the natural angle of the vortex.

Apart from the displaced wire, nothing about our setup differs substantially from two previous sets of experiments at temperatures below 400 mK [13, 17]. Our cylindrical cells have comparable dimensions to those in the earlier work. They are drilled or reamed, with no special polishing or other treatments, so the cell walls are probably no smoother than in the earlier experiments. Although our wires are the smallest used to date, our larger wires are within a factor of 2 of nearly all those previously reported. We believe the wire size improves the precession signatures only in a minor and indirect way. Most of our measurements are on vortex precession between  $n = 1$  and  $n = 0$ , although we also observe precession between  $n = 2$  and  $n = 1$ , as shown in Figure 1. In previous experiments slow transitions were usually found only between the higher circulation levels, with  $n = 1$  so stable that only steadily rotating the cryostat in the opposite sense to the vortex would dislodge it. From Figure 1, the  $n = 2$  to  $n = 1$  precession may be slightly noisier than that from  $n = 1$  to  $n = 0$ , but it is clearly visibly and far cleaner than previous  $^4\text{He}$  precession data [13]. The lower-circulation motion may be more regular because less vorticity remains in the cell. If so our smaller wires smooth the precession signature by favoring precession at  $n < 1$ , but are not a crucial feature of the current experiment.

## V. PINNING

In Schwarz' simulations, depinning events have characteristic signatures [14]. As shown in Figure 4, we find remarkably similar experimental signals, although at the onset of pin-

ning rather than at depinning. The precession oscillations at the left give way to faster, lower amplitude oscillations upon pinning. The energy dissipation also ceases, as expected once the vortex stops moving. The constant background signal that results is convenient for detecting the pinning oscillations experimentally. Upon depinning, any special signature is superimposed on both the oscillations from vortex precession and the linear change from decay of the trapped vorticity. In addition, if an external perturbation causes the depinning, other irregularities may occur in the decay signal just after the event.

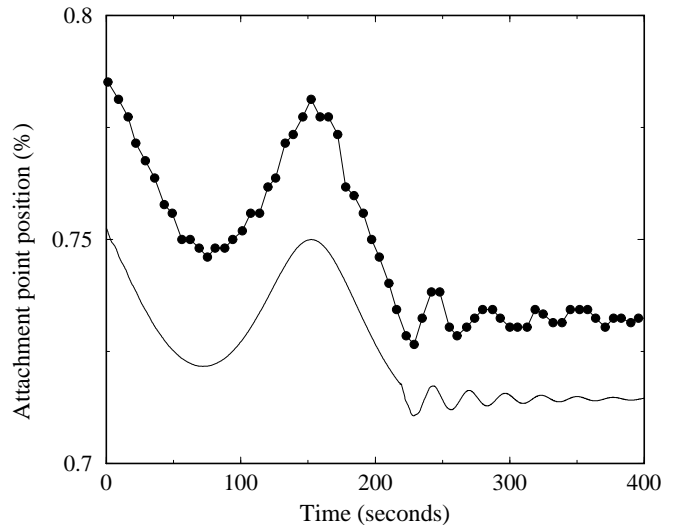


FIG. 4: Vortex becoming pinned during its precession. Top curve: measurements. Bottom curve: simulation for wire displaced 0.25 mm from cell center, pin site at  $\theta = 126^\circ$ , friction coefficient  $\alpha = 0.05$ .

The fast oscillations upon pinning arise from Kelvin waves on the free vortex segment. Kelvin originally treated of vortex waves on an infinite straight vortex with a sinusoidal distortion of wavelength  $k$  [18]. The distortion spirals about the core at frequency  $\omega = \kappa k^2 A / 4\pi$ . Here  $A \approx \ln(\frac{1}{ka})$  and  $a$  is the core radius. The boundary conditions of our experimental setup require a standing wave, which can be obtained by combining waves spiraling in opposite directions. With a node on the cell wall and maximum displacement on the wire, we require  $k = \frac{\pi}{2d}$  for the lowest mode, with  $d$  the distance from the wire to the pin site.

In Figure 4, the free vortex segment is longest at 131 seconds, and from this position travels for 85% of one period before pinning. From the amplitude of the precession oscillations, the estimated wire displacement is 0.25 mm. Then the distance from the wire to the pin site is 1.7 mm. The corresponding straight vortex mode has  $\omega = 0.11$  rad/s and period 58 seconds, substantially longer than the observed period of 37 seconds. The discrepancy comes largely from the effect of the cylindrical container, which forces the vortex to bend. The vortex line tension, or how the energy changes with shape, depends strongly on configuration. Indeed, even in a parallel-

plane geometry, boundary effects can lead to curvature that significantly changes the Kelvin oscillation period.

Pinning simulations for the present experimental geometry confirm the period change. As described in the previous section, we begin with a steadily precessing vortex and suddenly fix its free end. We choose the pin location to match the measured pin event. We note that, in keeping with our minimum angle simulations, the pin site in Figure 4. is near where the free vortex is longest. This is also true for the other long pinning events we observe. The simulations show oscillation of the free portion, coupled to motion of the attachment point up and down the wire, with period 29 seconds. The discrepancy between the simulation and experiment may come from our uncertain knowledge of the wire's displacement and the pin site's location in the cell. This is the clearest observation to date of a Kelvin wave on a single superfluid vortex line.

The damping of the Kelvin mode is many orders of magnitude too high to come from mutual friction with the normal fluid. Since one end is stationary at the wall, it is likely that the dissipation comes from the other end of the vortex moving up and down along the wire.

## VI. ASYMMETRIC OSCILLATIONS

Another feature predicted by Schwarz [14] is a slight asymmetry in the precession signature. The vortex velocity depends on the local fluid velocity. If the wire were centered in the cylinder, the fluid velocity would have no angular dependence. With the off-center wire, boundary effects increase the velocity where the wire is closest to the wall, so the vortex moves more quickly on this side. In the precession signal,

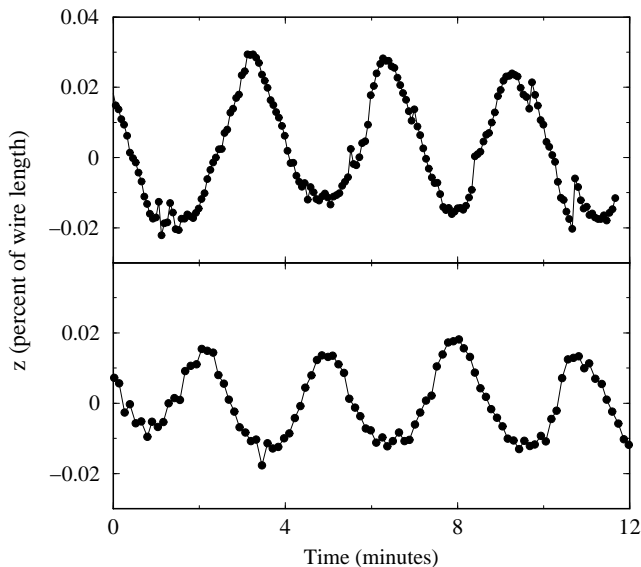


FIG. 5: Asymmetry in the precession oscillations, for wires A (upper) and C (lower). Note the relative roundedness of the troughs and sharpness of the peaks.

the fastest motion occurs at the top of each cycle, when the free vortex is short. The slowest precession is at the lowest trapped circulation, when the free vortex is longest. The result is slightly sharpened peaks and rounded troughs.

Figure 5 shows exactly this structure, for wires A and C. To remove the overall slope caused by energy loss, a line has been subtracted from each data set. Both the oscillation amplitude and the asymmetry are larger for wire A than for wire C, implying that wire A is farther off center. Observing the asymmetry in the precession signal is encouraging for the eventual goal of being able to track more complicated motion of a single vortex.

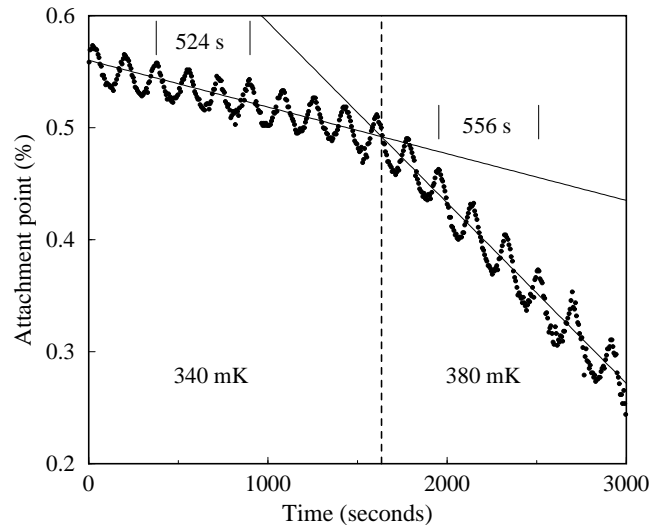


FIG. 6: Dependence of precession rate and dissipation on temperature. The solid lines are guides to the eye. The times for three periods are indicated, with the period increasing a small but noticeable amount with temperature.

## VII. TEMPERATURE DEPENDENCE

Another prediction involves temperature dependence. In addition to its interaction with the local velocity field, a vortex line feels a friction-like force proportional to its velocity. The friction force determines the energy loss, and hence the linear circulation decrease that appears along with vortex precession. Experimentally the friction coefficient  $\alpha$  depends strongly on temperature. Figure 6 illustrates the dramatic change in energy loss rate upon changing the temperature from 340 mK to 380 mK.

Computer simulations reveal that, while moving downward more rapidly, the vortex also precesses less quickly [14]. We now find experimentally that, as temperature increases, the dissipation rate and the precession period also increase. While the period change is small—only 6% in Figure 6—it is certainly outside our measurement error.

One difference between the simulations and experiments is the source of the friction. In the simulations, the dissipation comes from mutual friction, the interaction between the vortex and the normal fluid. This is not the case in experiments. In our temperature range, mutual friction is many orders of magnitude too small to account for the observed dissipation [19]. Instead, the most likely dissipation mechanism is the rubbing of the end of the vortex along the wall. It is interesting that the relationship between the precession rate and the dissipation holds nonetheless.

Schwarz finds that as dissipation increases, the precession rate slows [14]. In the limiting case of large dissipation, the vortex moves directly downward without precessing at all. Our wire B have this behavior; its circulation decay is very fast and exhibits no oscillations.

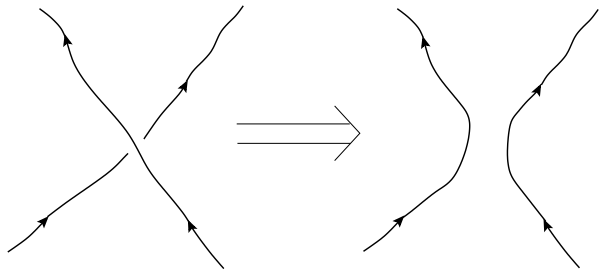


FIG. 7: Vortices reconnecting upon collision.

## VIII. INITIATING PRECESSION

In the work described here we usually shake the cryostat to initiate the vortex motion. However, in superfluid  $^3\text{He}$  [12] and occasionally in our present measurements, a trapped vortex may leave the wire without deliberate external perturbation. How the unwinding process begins remains unknown. Schwarz suggests that a free vortex in the cell collides with the  $n = 1$  vortex along the wire [14]. Close approach of vortices often leads to a runaway attraction ending in reconnection [15], illustrated in Figure 7. The vortices are cut at the crossing point, and the segments leading in and out are reattached in the opposite way. A reconnection involving one free vortex and one trapped around the wire would create two partially attached vortices.

Figure 8 shows what we believe is two unwinding partial vortices. The cryostat was rotated immediately before the data pictured. From the irregular circulation signal for the first few minutes we hypothesize that a jumble of vortices pervades the cell. After 10 minutes precession begins, with the usual period near three minutes and large amplitude oscillations. This is consistent with two partially attached vortices, which are on the same side of the wire at the same time. Additional structure appears in the decay, and by 20 minutes the frequency has doubled, with the amplitude dropping dramatically. One explanation is that the two precessing vortices are now out of

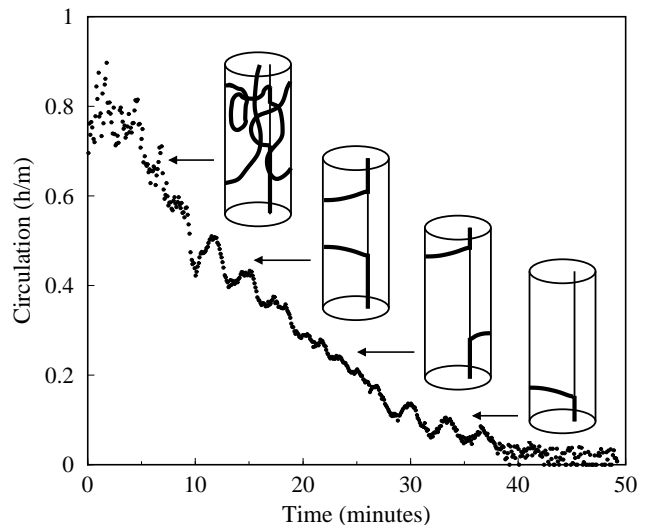


FIG. 8: Vortices unwinding from both ends of the wire simultaneously. The schematics illustrate possible vortex configurations at the times indicated.

phase. If one is long while the other is short, their effects on the trapped vortex length partly cancel, reducing the oscillation amplitude. (The cancellation cannot be complete. Since the superfluid velocity field, and hence the precession rate, depends on the position within the cell, the two vortices cannot remain perfectly out of phase with each other.) The frequency doubling occurs because the two vortices attain an equivalent configuration, with their roles transposed, after each traverses only half of the cell. Finally, after 30 minutes, the oscillations return to the usual precession frequency. These are cleaner than the large oscillations earlier in the decay, and signify that one of the vortices has completed its unwinding, returning the cell to a single-vortex situation.

We have seen one other similar signature. Since the vortex precession is usually much cleaner than this, we believe that our more typical signatures involve only one partially attached vortex. This means that the unwinding process generally does *not* start from a free vortex collision, since even unwinding that begins without shaking rarely leads to signatures like that of Figure 8. We have calculated numerically the energy in the flow field for two partially attached vortices if they are on the same or opposite sides of the cell. The out of phase configuration is energetically favorable, which is consistent with its appearance in our observations. We have not yet investigated how the vortices change from in phase to out of phase.

## IX. CONCLUSIONS

We present data on smooth vortex precession in superfluid  $^4\text{He}$ . A key difference between our work and other vibrating wire measurements is that our wires are located substantially away from the axis of the container. We verify several numerical predictions for precession signatures: behavior at pinning

events, the oscillation asymmetry from the off-center wire, and the relationship between the vertical motion of the trapped vortex and its precession period. The repeatable, smooth vortex precession can serve as a probe in further experiments on dynamics of one or a few vortices.

Our measurements also address the question of how the precession begins. We see a distinctive signature for two partially attached vortices. Its absence in the bulk of our measurements means that this configuration rarely initiates the precession. A more common situation appears to be a partially dislodged vortex which may return to the wire or change to terminate on the cell wall. Since many of our vortex decays begin with literally shaking the cryostat, our typical detachment mechanism may differ from behavior in the absence of such strong external perturbations. Better controlled studies of how the vortex first comes off the wire remain to be done.

### REFERENCES

- [1] H.J. Lugt, *Vortex Flow in Nature and Technology* (John Wiley & Sons, New York, 1983).
- [2] L. Ying and P. Zhang, *Vortex methods* (Science Press, Beijing, 1997).
- [3] S.M. Belotserkovskii and I.K. Lifanov, *Method of discrete vortices* (CRC Press, Boca Raton, 1993).
- [4] H. Yamade and T. Matsui, "Mutual slip-through of a pair of vortex rings," *Phys. Fluids* **22**, 1245 (1979).
- [5] S.I. Green, *Fluid Vortices* (Kluwer Academic Publishers, Dordrecht, 1995), Chapter 1.
- [6] B.P. Anderson, P.C. Haljan, C.E. Wieman, and E.A. Cornell, "Vortex precession in Bose-Einstein condensates: Observations with filled and empty cores," *Phys. Rev. Lett.* **85**, 2857 (2000).
- [7] M. Breitwisch and D. Finnemore, "Pinning of a single Abrikosov vortex in superconducting Nb thin films using artificially induced pinning sites," *Phys. Rev.* **B62**, 671 (2000) and references therein.
- [8] W.F. Vinen, "The detection of a single quantum of circulation in liquid helium II," *Proc. Roy. Soc. London* **A260**, 218 (1961).
- [9] S.C. Whitmore and W. Zimmermann, Jr., "Observation of quantized circulation of superfluid helium," *Phys. Rev.* **166**, 181 (1968).
- [10] J.C. Davis, J.D. Close, R. Zieve, and R.E. Packard, "Observation of quantized circulation in superfluid  $^3\text{He-B}$ ," *Phys. Rev. Lett.* **66**, 329 (1991).
- [11] R.J. Zieve et al., "Precession of a single vortex line in superfluid  $^3\text{He}$ ," *Phys. Rev. Lett.* **68**, 1327 (1992).
- [12] R.J. Zieve et al., "Investigation of quantized circulation in superfluid  $^3\text{He-B}$ ," *J. Low Temp. Phys.* **91**, 315 (1993).
- [13] R.J. Zieve, J.D. Close, J.C. Davis, and R.E. Packard, "New experiments on the quantum of circulation in  $^4\text{He}$ ," *J. Low Temp. Phys.* **90**, 243 (1993).
- [14] K.W. Schwarz, "Unwinding of a single quantized vortex from a wire," *Phys. Rev.* **B47**, 12030 (1993).
- [15] K.W. Schwarz, "Three-dimensional vortex dynamics in superfluid  $^4\text{He}$ : Line-line and line-boundary interactions," *Phys. Rev.* **B31**, 5782 (1985).
- [16] R.J. Zieve and L.A.K. Donev, "Stable Vortex Configurations in a Cylinder," *J. Low Temp. Phys.* **121**, 199 (2000).
- [17] P.W. Karn, D.R. Starks, and W. Zimmermann, Jr., "Observation of quantization of circulation in rotating superfluid  $^4\text{He}$ ," *Phys. Rev.* **B21**, 1797 (1980).
- [18] Thomson, W., "Vibrations of a columnar vortex," *Phil. Mag.* **10**, 155 (1880).
- [19] G.W. Rayfield and F. Reif, "Quantized vortex rings in superfluid helium," *Phys. Rev.* **136**, A1194 (1964).